

MICROSTRUCTURES AND MECHANICAL PROPERTIES OF  
SPUTTERED Cu/Cr MULTILAYERS

A. MISRA, H. KUNG, T.E. MITCHELL, T.R. JERVIS and M. NASTASI,  
Los Alamos National Laboratory, MS K765, Los Alamos, NM 87545.

RECEIVED

APR 06 1998

CONF-971201-- OSTI

## ABSTRACT

The microstructures and mechanical properties of Cu/Cr multilayers prepared by sputtering onto {100} Si substrates at room temperature are presented. The films exhibit columnar grain microstructures with nanoscale grain sizes. The interfaces are planar and abrupt with no intermixing, as expected from the phase diagram. The multilayers tend to adopt a Kurdjumov-Sachs (KS) orientation relationship:  $\{110\}\text{Cr} // \{111\}\text{Cu}$ ,  $\langle 111 \rangle \text{Cr} // \langle 110 \rangle \text{Cu}$ . The hardness of the multilayered structures, as measured by nanoindentation, increase with decreasing layer thickness for layer thicknesses ranging from 200 nm to 50 nm, whereas for lower thicknesses the hardness of the multilayers is independent of the layer thickness. Dislocation-based models are used to interpret the variation of hardness with layer periodicity. The possible effects of factors such as grain size within the layers, density and composition of films and residual stress in the multilayers are highlighted. Comparisons are made to the mechanical properties of sputtered polycrystalline Cu/Nb multilayers which, like Cu/Cr, exhibit sharp fcc/bcc interfaces with no intermixing and a KS orientation relationship, but have a small shear modulus mismatch.

MASTER

## INTRODUCTION

The mechanical properties of fine scale microstructures such as nanocrystalline materials [1], structures produced by wire drawing of metal-metal composites [2,3] and multilayered thin films processed by sputtering or evaporation [4-6], have been the subject of many recent investigations. In addition to the numerous potential applications of these materials such as wear resistant multilayered nitride coatings [5], and high strength and high electrical conductivity composite wires like Cu-Nb [2] and Cu-Cr [3], there is a fundamental interest in understanding the deformation and fracture behavior of such materials [7]. These fine scale composite materials typically exhibit strength levels significantly higher than what would be expected by a rule-of-mixtures prediction, and often the flow stresses at room temperature can approach 1/2 to 1/3 of the theoretical strength of the order of  $G/30$  where  $G$  is the shear modulus [7]. For multilayered thin films, the increase in strength with decreasing bilayer period has been explained by a number of different mechanisms such as Hall-Petch hardening, Koehler hardening [8] and Orowan bowing of dislocations between layers, as discussed in a recent review article by Was and Foecke [9]. For epitaxial multilayered films, the only microstructural scale of significance is the layer thickness ( $h$ ) but in polycrystalline multilayered thin films, the grain size ( $d$ ) within the layers may also play an important role in influencing the hardness, especially if  $d < h$ .

In the present investigation, the microstructures and mechanical properties of Cu/Cr nanolayered composite films prepared by sputter deposition are studied. Cu and Cr have no significant mutual solubility, and are expected to form sharp interfaces. The shear modulus of Cr is ~2.5 times higher than that of Cu. The variation of the hardness of Cu/Cr nanolayered composites as a function of layer thickness is interpreted using dislocation-based models and microstructures within the layers.

DISTRIBUTION OF THIS DOCUMENT IS UNLIMITED *ph*

## EXPERIMENTAL PROCEDURES

Cu/Cr multilayers with layer thicknesses ranging from 1 nm to 200 nm, and single layer Cu and Cr films with thicknesses ranging from 25 nm to 1  $\mu\text{m}$  were dc sputter deposited at room temperature on {100} Si wafers cleaned by etching in 10% HF solution. The deposition was carried out under 5 mtorr Ar pressure at 300 W of power to the target, after pumping down to a vacuum of  $< 1 \times 10^{-8}$

19980504 049

## **DISCLAIMER**

This report was prepared as an account of work sponsored by an agency of the United States Government. Neither the United States Government nor any agency thereof, nor any of their employees, makes any warranty, express or implied, or assumes any legal liability or responsibility for the accuracy, completeness, or usefulness of any information, apparatus, product, or process disclosed, or represents that its use would not infringe privately owned rights. Reference herein to any specific commercial product, process, or service by trade name, trademark, manufacturer, or otherwise does not necessarily constitute or imply its endorsement, recommendation, or favoring by the United States Government or any agency thereof. The views and opinions of authors expressed herein do not necessarily state or reflect those of the United States Government or any agency thereof.

torr. The layer sequence was Si/Cr/Cu with equal thicknesses of Cr and Cu layers. The total thickness of the multilayered thin films was  $\sim 1 \mu\text{m}$ . The deposition rates were  $\sim 1 \text{ nm/s}$  for Cu and  $\sim 0.6 \text{ nm/s}$  for Cr. Characterization of the as-deposited films was performed using transmission electron microscopy (TEM) and Rutherford backscattering spectroscopy (RBS). TEM was performed on a Philips CM30 microscope at 300 kV. Standard RBS spectra were obtained using 2 MeV  $\text{He}^+$  ions. Density of Cr films was determined by a combination of profilometry and RBS techniques. A Cu capping layer of  $\sim 3 \text{ nm}$  was put on single layer Cr films used for nano-indentation and RBS to prevent build up of surface oxide. The residual stress in the single layered films and multilayers was measured using standard curvature technique. The hardness and indentation modulus of the multilayers and  $1 \mu\text{m}$  single layer Cu and Cr films were measured using an indentation load-depth sensing apparatus, commercially available as Nano Indenter® II. Continuous stiffness technique was used for nano-indentation with a displacement rate of  $2 \text{ nm/s}$ . The nominal indentation depth was  $150 \text{ nm}$ .

## RESULTS

The microstructures of the single layered Cu and Cr films and Cu/Cr multilayers are shown in Fig. 1. A plan view TEM micrograph of a  $1 \mu\text{m}$  Cu film is shown in Fig. 1(a). Note the polycrystalline microstructure with a high density of twins within the grains. For  $1 \mu\text{m}$  Cu film, the grains were almost equiaxed with a weak  $\langle 111 \rangle$  texture. Cr films had columnar-grain microstructures as shown in Fig. 1 (b), which is a cross-section TEM micrograph of a  $1 \mu\text{m}$  Cr film. The grain boundaries in Cr films often exhibited Fresnel contrast indicating that the grain boundaries may have a non-equilibrium, porous structure. A cross-section TEM micrograph of a  $100 \text{ nm}/100 \text{ nm}$  Cu/Cr multilayer is shown in Fig. 1(c), with the corresponding diffraction pattern in Fig. 1(d). The interfaces are flat with no waviness of the layers. Note the columnar-grain microstructure of the Cr film with an aspect ratio of  $\sim 6$  for layer thickness of  $100 \text{ nm}$ . The aspect ratio of Cu grains in  $100 \text{ nm}$  layer is  $\sim 2$ , indicating that the grains are less equiaxed as compared to  $1 \mu\text{m}$  Cu film. The grain sizes in both layers were found to decrease with decreasing layer thickness. The diffraction pattern (Fig. 1(d)) is ring-type consistent with the nanometer-scale grain sizes in the multilayers. An indication of the  $\{110\}\text{Cr} // \{111\}\text{Cu}$  texture may be inferred from the diffraction pattern, which is consistent with the observation of a Kurdjumov-Sachs orientation relationship:  $\{110\}\text{bcc} // \{111\}\text{fcc}$ ,  $\langle 111 \rangle\text{bcc} // \langle 110 \rangle\text{fcc}$  in sputtered Cu/Nb multilayers [4].

Measurements of the area atomic density (number of atoms per unit area) by RBS and the film thickness by profilometry of single layered Cr films were used to calculate the density. It was found that the density is typically  $\sim 97\text{-}98\%$  of the theoretical density of Cr, consistent with other investigations on dc sputtered Cr films at room temperature with no substrate bias [10]. A RBS spectrum of a Cr film  $\sim 0.6 \mu\text{m}$  thick, with a Cu capping layer, is shown in Fig. 2, along with the simulation of the spectrum (shown as a dotted line) performed using the software RUMP [11]. The oxygen content in the Cr film was determined to be  $< 0.01 \text{ at.}\%$ .

The variation of the intrinsic residual stresses in Cu/Cr multilayers with layer thickness, and in Cr and Cu single layer films with film thickness are shown in Fig. 3. Note that the residual stresses are tensile, and appear to peak at  $\sim 50 \text{ nm}$  layer thickness in the multilayers and Cr films. The residual stresses in Cu films are about an order of magnitude lower than that in Cr films and hence, the intrinsic stresses in the Cr layer are expected to control the residual stress behavior of Cu/Cr multilayers.

The indentation modulus of the Cu film was measured as  $137 \pm 6 \text{ GPa}$ , which is in reasonable agreement with the modulus of bulk Cu. The indentation modulus measured for the Cr film exhibited much larger scatter,  $179\text{-}230 \text{ GPa}$ , and  $\sim 10\text{-}20\%$  lower modulus than bulk Cr. The indentation modulus of the multilayers was approximately the average of Cu and Cr indentation moduli and independent of the layer thickness. From the measured indentation moduli, the shear and Young's moduli were calculated using literature values of Poisson's ratio as follows:  $E_{\text{Cu}} = 125 \text{ GPa}$ ,  $G_{\text{Cu}} = 47.6 \text{ GPa}$ ,  $E_{\text{Cr}} = 220 \text{ GPa}$  and  $G_{\text{Cr}} = 92 \text{ GPa}$ . The hardness (H) of the multilayers was measured up to a total indentation depth of  $150 \text{ nm}$ . For indentation depths higher than  $50$

nm, the hardnesses of multilayers approached saturation values with further increase in depth of indentation. Hall-Petch (H-P) plots of hardness vs.  $h^{-1/2}$  for total indentation depths of 85 nm and 135 nm are shown in Fig. 4(a). The hardness at 135 nm depth is slightly higher than that at 85 nm depth for all samples, but the difference is insignificant since the error bars overlap. The average rule of mixtures hardness was  $\sim 4$  GPa. For  $50 \text{ nm} \leq h \leq 200 \text{ nm}$ , the variation of H with  $h^{-1/2}$  is linear. A transition region is noted for  $10 \text{ nm} < h < 50 \text{ nm}$  and for  $h \leq 10 \text{ nm}$ , H reaches a plateau at  $\sim 6.8$  GPa. Almost identical plots are obtained, Fig. 4(b), if H is plotted as a function of  $h^{-1} \ln(h)$ . These results are discussed below using various dislocation plasticity models.

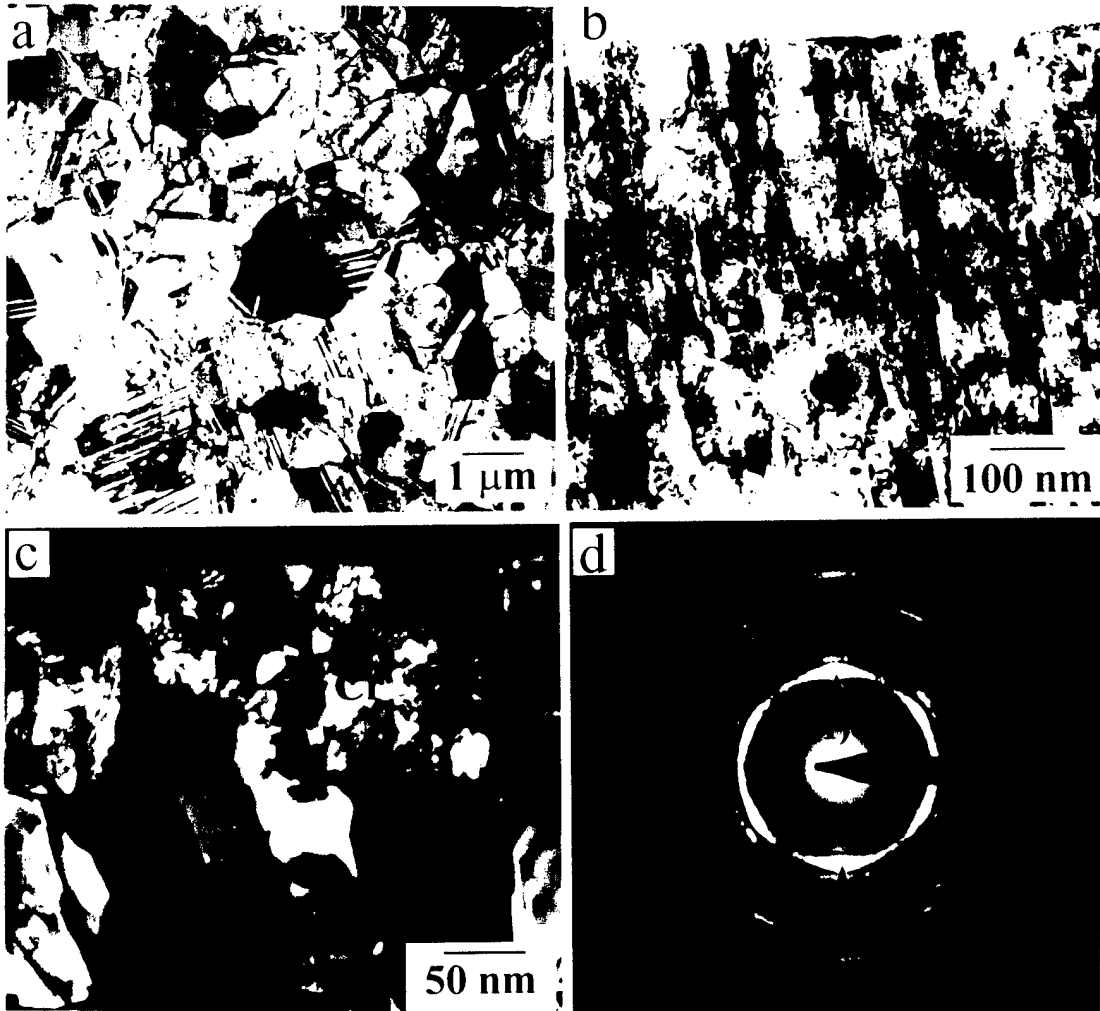


Fig. 1(a) Plan view TEM micrograph of a 1  $\mu\text{m}$  Cu film, (b) Cross-section TEM micrograph of a 1  $\mu\text{m}$  Cr film, (c) Cross-section dark field TEM micrograph of a 100nm/100nm Cu/Cr multilayer, (d) selected area diffraction pattern of the image in (c).

## DISCUSSION

### Residual Stress

Tensile residual stresses of about the same magnitude and variation with film thickness to that shown in Fig. 3, have been reported for single layer Cr films deposited at room temperature [10,12]. The development of an intrinsic tensile stress in sputtered metallic thin films during growth is usually attributed to the densification of the film [12]. It is believed that the material is deposited in a metastable state, e.g., non-equilibrium, porous grain boundaries, and as the film grows thicker, subsequent atomic arrangements tend to produce more equilibrium and compact

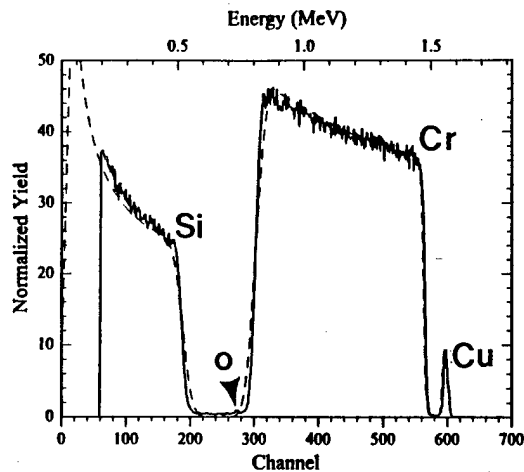


Fig. 2. RBS spectrum from a Cr film  $\sim 0.6 \mu\text{m}$  with a 3 nm Cu capping layer.

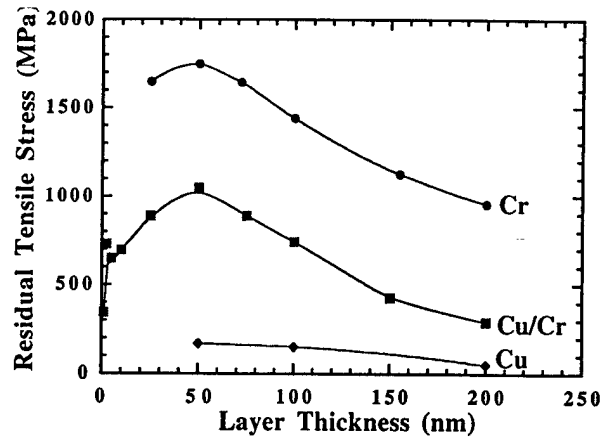


Fig. 3. Residual stresses in Cu/Cr multilayers as a function of layer thickness, and single layer Cr and Cu films as a function of film thickness

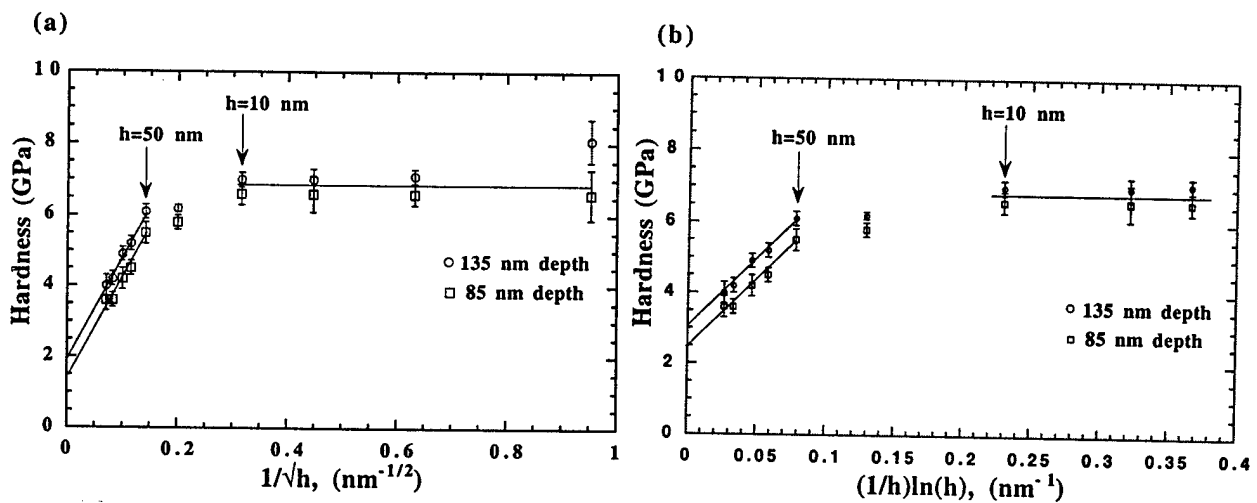


Fig. 4. Hardness of Cu/Cr multilayers plotted as a function of (a)  $h^{-1/2}$  and (b)  $h^{-1}\ln(h)$ , where  $h$  is the layer thickness.

grain boundaries. The densification would result in shrinkage of the film if it were not attached to the substrate. However, the constraint by the substrate leads to the development of a biaxial tensile stress. The observations of Fresnel fringes in TEM images of grain boundaries in Cr films and lower density and modulus of Cr film as compared to bulk Cr are consistent with this explanation. Since the stresses in the single layer Cu films are very low, the intrinsic stresses in the Cr layers are expected to control the residual stresses in the multilayers. Another source of stress in multilayers is the interface [13]. It has been shown that for multilayers of two metals A and B, the total stress as measured by the substrate curvature technique,  $\sigma_T$  is given as [13]:

$$\sigma_T = \langle \sigma \rangle + 2\gamma/\lambda$$

where  $\langle \sigma \rangle = (\sigma_A + \sigma_B)/2$ , and  $\sigma_A$ ,  $\sigma_B$  are in-plane stresses in layers A and B respectively obtained from X-ray strain measurements,  $\gamma$  is the interface stress and  $\lambda$  is the bilayer repeat period. In this investigation, X-ray strain measurements were not performed. However, the residual stresses in the Cu/Cr multilayers, were found to be very close to the average of the intrinsic stresses in the single layered Cr and Cu films. Hence, it appears that the interface stress may not be a major contributor to the total stress in the multilayer.

## Hardness

A linear fit through the hardness vs  $h^{-1/2}$  data for  $50 \text{ nm} \leq h \leq 200 \text{ nm}$  yields a slope of  $0.31 \text{ MPa}\cdot\text{m}^{1/2}$  and intercept of  $1.8 \pm 0.2 \text{ GPa}$ . The intercept is almost equal to the hardness of  $1 \mu\text{m}$  Cu film,  $1.6 \pm 0.1 \text{ GPa}$ . The H-P plot of hardness data of sputtered Cu-Nb multilayers also yielded an intercept equal to the hardness of  $1 \mu\text{m}$  Cu film [4]. However, in Cu-Nb, the H-P slope was  $0.15 \text{ MPa}\cdot\text{m}^{1/2}$  which is almost identical to the slope in bulk polycrystalline Cu [14]. In Cu-Cr, the H-P slope of  $0.31 \text{ MPa}\cdot\text{m}^{1/2}$  is still closer to that of bulk Cu than Cr which has a H-P slope of  $\sim 0.90 \text{ MPa}\cdot\text{m}^{1/2}$  in bulk as well as electrodeposited conditions with grain sizes as small as  $0.15 \mu\text{m}$  [15]. Thus, increased hardness in the multilayered structures can be attributed to grain boundaries within the layers and Cu/Cr interfaces in the  $50 \text{ nm} \leq h \leq 200 \text{ nm}$  range.

For  $h \leq 10 \text{ nm}$ , there is no detectable variation in hardness with  $h$ , which is different from Cu/Nb where hardness was found to be weakly dependent on  $h$  in the range  $1 \text{ nm} \leq h \leq 50 \text{ nm}$  [4]. The hardness behavior in this range of  $h$  was interpreted in terms of Orowan bowing of dislocations between the layers in Cu-Nb [4]. Based on a Haasen plot analysis of hardness data, Tambwe *et al.* [16] have suggested that for polycrystalline multilayered thin films like Cu/Nb with no shear modulus mismatch, the variation of hardness with  $h$  in the entire range, i.e.  $1 \text{ nm} \leq h \leq 500 \text{ nm}$ , may be explained by a single mechanism involving Orowan bowing of dislocations where hardness increases with decreasing grain size within the layer according to  $d^{-1}\ln(d)$  [16].

The plot of  $H$  vs  $h^{-1}\ln(h)$  for Cu/Cr (Fig. 4(b)) shows that data for  $50 \text{ nm} \leq h \leq 200 \text{ nm}$  fall on a straight line with slope of  $41 \text{ GPa}\cdot\text{nm}$  and an intercept of  $2.8 \pm 0.3 \text{ GPa}$ . Again, hardness reaches a plateau for lower  $h$ . Similar plots with approximately the same slope were observed for  $H$  vs  $d^{-1}\ln(d)$  where  $d$  was taken as the grain size within either Cu or Cr layer. The slope of such plots should scale with  $3Gb/2\pi(1-\nu)$  where  $b$  is the Burgers vector,  $\nu$  is the Poisson's ratio and the factor of 3 is to convert yield stress to hardness [4]. Estimates of  $3Gb/2\pi(1-\nu)$  using  $G_{\text{Cu}}$  and  $G_{\text{Cr}}$  resulted in values of  $8.4 \text{ GPa}\cdot\text{nm}$  and  $13.7 \text{ GPa}\cdot\text{nm}$  respectively, both significantly lower than the slope of  $41 \text{ GPa}\cdot\text{nm}$  measured for the linear fit in Fig. 4(b). Thus, the H-P model appears to provide more reasonable fit to the hardness data for  $50 \text{ nm} \leq h \leq 200 \text{ nm}$ .

For  $h < 50 \text{ nm}$ , hardness is almost independent of  $h$  which cannot be explained either by H-P or Orowan bowing models. A plateau of  $H$  below a critical  $h$  is not uncommon in multilayers where there is a large shear modulus mismatch between the two layers, such as Ag/Cr [6], Al-Cu [17] and several nitride superlattices [5]. The saturation yield stress may be estimated using the Koehler model [8], based on the image force on dislocations, modified by Lehoczky for a three-layer (two-interface) case. Calculations involving multiple images and interfaces suggest that the three layer case gives a reasonable estimate of the image force [18]. For multilayers having layer thicknesses below the critical value required for the operation of Frank-Read sources, the yield strength for iso-strain conditions may be estimated according to [17]:

$$\sigma_y = (V_{\text{Cu}} + V_{\text{Cr}}E_{\text{Cr}}/E_{\text{Cu}})(G_{\text{Cu}}/8\pi)(\alpha) + \sigma_i$$

where  $\alpha$  is the shear modulus mismatch,  $(G_{\text{Cr}} - G_{\text{Cu}})/(G_{\text{Cr}} + G_{\text{Cu}})$ ,  $V_i$  and  $E_i$  are volume fraction and Young's modulus respectively of the layer  $i$  and  $\sigma_i$  is the lattice friction stress in the Cu layer which is taken as the hardness of  $1 \mu\text{m}$  Cu film. Taking  $V_i$  as 0.5 and elastic constants as mentioned earlier,  $\sigma_y$  is calculated as  $1.37 \text{ GPa}$  which corresponds to a hardness of  $\sim 4 \text{ GPa}$ , assuming  $H = 3\sigma_y$ . The same calculation using literature values of bulk polycrystalline Cu and Cr results in a saturation hardness of  $5.3 \text{ GPa}$ . The experimentally observed hardness plateau is  $\sim 6.8 \text{ GPa}$ . Thus, the model underestimates the hardness plateau. Lehoczky found good agreement of the model predictions with experimentally measured tensile yield strength plateaus in Al-Cu and Al-Ag laminates [17]. A possible reason for the disagreement between the model predictions and experimental data is that the model estimates tensile yield strength while the experiment measures hardness by nanoindentation. Recently, it was shown that nanoindentation hardness for annealed single crystals of Cu decreased from  $\sim 1.8 \text{ GPa}$  for indentation depth of  $\sim 0.2 \mu\text{m}$  to  $0.8 \text{ GPa}$  for indentation depth of  $\sim 2 \mu\text{m}$  [19]. Nanoindentation of strain-hardenable metals may result in high

hardnesses at small depths due to the geometrically necessary dislocations created [19]. Further, the assumed relationship of  $H = 3\sigma_y$  may not be valid for low depth (< 150 nm) nanoindentation of metals. For example, the nanoindentation hardness of 1  $\mu\text{m}$  Cu film, which had a grain size of  $\sim 1 \mu\text{m}$ , was measured as  $1.6 \pm 0.1 \text{ GPa}$ . Using the  $H = 3\sigma_y$  conversion, this should correspond to a yield strength of  $\sim 533 \text{ MPa}$ , when in fact bulk polycrystalline Cu of 1  $\mu\text{m}$  grain size may have a yield strength of only  $\sim 140 \text{ MPa}$  [14]. Thus, tensile yield strength data may be needed on these multilayers to allow better comparison with the dislocation plasticity models. Further, it has been pointed out that the continuum plasticity considerations such as stress transfer to the harder, less-deforming phase (Cr) may explain a portion of the stress elevation observation in fine-scale structures [7]. Again, tensile yield strength data are more suitable than nanoindentation hardness data to model such effects.

## SUMMARY

Sputtered Cu/Cr multilayers have polycrystalline microstructures with nanometer scale grain sizes. The residual stresses are found to be tensile with a peak value of 1050 MPa at layer thickness of 50 nm which can largely be attributed to the intrinsic tensile stress in the Cr layer. The intrinsic tensile residual stress is believed to be associated with the densification of the film during growth. The hardness of the multilayers in the layer thickness range of 50 nm - 200 nm is explained by Hall-Petch model with grain boundaries and interfaces as barriers. The plateau in the hardness for layer thickness < 50 nm is interpreted by the Koehler model based on the shear modulus mismatch between the layers.

## ACKNOWLEDGEMENTS

This research is funded by Los Alamos National Laboratory. The assistance of J. Tesmer, IBML, with RBS experiments is acknowledged.

## REFERENCES

1. M. Nastasi, D. Parkin and H. Gleiter, Mechanical Properties and Deformation Behavior of Materials Having Ultra-Fine Microstructures, Kluwer, Dordrecht, 1993.
2. W.A. Spitzig, A.R. Pelton and F.C. Laabs, *Acta Metall.*, **35**, p 2427, 1987.
3. K. Adachi, S. Tsubokawa, T. Takeuchi and H.G. Suzuki, *J.Jp.Inst.Met.*, **61**, p 397, 1997.
4. T.E. Mitchell, Y.C. Lu, A.J. Griffin, M. Nastasi and H. Kung, *J.Am.Cer.Soc.*, **80**, p 1673, 1997.
5. S.A. Barnett and M. Shinn, *Ann. Rev. Mater. Sci.*, **24**, p 481, 1994.
6. G.R. English, G.F. Simenson, B.M. Clemens and W.D. Nix, *Mat. Res. Soc. Sym. Proc.*, **356**, p 363, 1995.
7. J.D. Embury and J.P. Hirth, *Acta Metall. Mater.*, **42**, p 2051, 1994.
8. J.S. Koehler, *Phys. Rev. B*, **2**, p 547, 1978.
9. G.S. Was and T. Foecke, *Thin Solid Films*, **286**, p 1, 1996.
10. J.C. Lin, R.A. Hoffman and N.J. Panseri, *Mat.Manf.Proc.*, **12**, p 329, 1997.
11. L.R. Doolittle, Ph.D. Thesis (Cornell University, Ithaca, NY, 1987).
12. M.F. Doerner and W.D. Nix, *CRC Crit.Rev.Sol.St.Mat.Sci.*, **14**, p 25, 1988.
13. J.A. Ruud, A. Witvrouw and F. Spaepen, *J.Appl.Phys.*, **74**, p 2517, 1993.
14. N. Hansen and B. Ralph, *Acta Met.*, **30**, p 411, 1982.
15. C.P. Brittain, R.W. Armstrong and G.C. Smith, *Scripta Met.*, **19**, p 89, 1985.
16. M.F. Tambwe, D.S. Stone, M. Nastasi, A.J. Griffin, H. Kung and Y.C. Lu, *J.Mater.Res.*, submitted.
17. S.L. Lehoczky, *J.Appl.Phys.*, **49**, p 5479, 1978.
18. S.V. Kamat, J.P. Hirth and B. Carnahan, *Scripta Met.*, **21**, p 1587, 1987.
19. W.D. Nix, *Mat.Sci.Eng.*, **A234-236**, p 37, 1997.

M98004390



Report Number (14) LA-UR--97-5029  
CONF-971201--

Publ. Date (11) 199803

Sponsor Code (18) DOE/MA, XF

UC Category (19) UC-904, DOE/ER

DOE